

# ALMA Memo 306

## A Dual-Polarization Double Sideband Quasi-Optical System for High Frequency ALMA Receivers

W. Grammer  
National Radio Astronomy Observatory

May 2, 2000

### Abstract

A double sideband receiver using a dual-polarization, dual-beam interferometer for LO diplexing is suggested as a suitable scheme for the high frequency ALMA bands. The bandpass characteristics of the diplexer, including ohmic loss of the grids and mirrors and diffraction losses are analyzed. The integrated LO noise present in the signal passband is also determined.

## 1 Introduction

The system described here is based on an amplitude-division interferometer, using a beam-splitting wire grid that operates on both linear polarizations. The advantage of the proposed configuration over one based on the Martin-Puplett interferometer is essential simplicity. One tuning mechanism serves both polarizations, and the system is compact and simple. The advantages of the Martin-Puplett style system are preserved: low-loss LO injection, rejection of noise on the LO at the signal frequency and balanced double sideband operation. The primary limitation of this system is the limited bandwidth of the splitting grid; a separate diplexer would be needed for each receiver band. It is envisioned that a possible application would be to have a multiplier chain associated with each diplexer and to have both multiplier and diplexer located outside the dewar.

The situation with regard to the production receivers for ALMA has been changing rapidly in the past few months. The results of various studies ([1],

[2], [3], [4]), together with recommendations from both the ALMA Systems Group and the ALMA Scientific Advisory Committee (ASAC) open the possibility of DSB receivers providing acceptable performance for ALMA. The adoption of DSB receivers would result in simplification and the realization of receivers with existing components.

This memorandum was written with this requirement in mind and is mainly a resurrection of some old ideas together with a fairly complete analysis. However, Kerr [5] has recently suggested that an LO injection scheme based on a waveguide hybrid junction may now be feasible at the higher ALMA receiver bands, eliminating the need for a quasi-optical diplexer. Nevertheless, the system presented in this memo represents a viable alternative.

## 2 Description

The basic dual-beam interferometer, described by Payne and Wordeman [6] is shown in Figure 1. A functionally equivalent but more elaborate version is given in Figure 2. Unlike the simpler configuration, the path length difference may be reduced to zero without obstructing the beams. Both the above use dual-polarization beam splitting grids as in [7]. The injected LO polarization is oriented 45 degrees to the grid wires, splitting the LO power equally into both polarizations. Within the dewar, a wire grid separates the two principal polarizations of the signal and LO, and a cold load provides a low-noise termination to the cross-polarization response of the mixer feeds.

## 3 Analysis

The dual-beam interferometer has been analyzed in detail by Goldsmith [8]; these results will be applied to the current design. Several assumptions are made in the analysis. The signal and LO paths are assumed to be pure Gaussian fundamental-mode beams. If scalar feedhorns are used and beam truncation is minimized, this is valid to a first order. Also, the incident beam from the subreflector is assumed well-coupled to the mixer feeds; mismatch and dielectric loss in the collimating lens is neglected. While important, this is a design aspect of the receiver separate from the diplexer, and will not be addressed in this memo.

As an example, the ALMA Band 8 receiver (602-720 GHz) will be assumed in the following analysis. An IF band from 4-12 GHz is also assumed.

### 3.1 Design of the Beam Splitter

The beam splitter/combiner consists of an overlapping grid of very fine tungsten wires at a constant spacing, gold plated to reduce ohmic loss. Each set of wires can be modeled fairly accurately as a simple two-port network with shunt impedance  $Z_g = R_L + jX_L$  and terminating impedance  $Z_o$ , where  $R_L$  is the ohmic loss and  $X_L$  a simple inductive reactance. To a first order, the two principal polarizations can be handled independently, as one array of wires is virtually transparent to the polarization acting on the other.

For an  $E$ -plane polarization parallel to the wires with angle of incidence  $\theta$ , Marcuvitz [9] gives the normalized grid reactance as

$$\frac{X_L}{Z_o} = \frac{g \cos \theta}{\lambda} \left\{ \ln \frac{g}{2\pi a} + \frac{1}{2} \sum_{m=-\infty}^{\infty} \left[ \frac{1}{\sqrt{m^2 + \frac{2mg}{\lambda} \sin \theta - \left(\frac{g \cos \theta}{\lambda}\right)^2}} - \frac{1}{|m|} \right] \right\}, m \neq 0 \quad (1)$$

where  $g$  is the wire spacing,  $a$  the wire radius,  $Z_o$  the free-space wave impedance and  $\lambda$  the wavelength, with  $g(1 + \sin \theta)/\lambda < 1$ . Figure 3 shows the reactance at midband (660 GHz,  $\lambda=454.2\mu\text{m}$ ) versus  $g$  for 0.001" diameter wire ( $a=12.7\mu\text{m}$ ), at 45 degree incidence. Neglecting loss for the moment, it can be shown that for an equal split between transmitted and reflected power,  $X_L/Z_o=0.5$ . From the graph, this corresponds to a spacing  $g$  of **214.2 $\mu\text{m}$** .

### 3.2 Ohmic Losses in the Optics

Loss in the splitter is derived from the resistive loss of the wires. From [8], the fraction of power absorbed is

$$A_s = \frac{P_{absorb}}{P_{incid}} = \frac{R_L Z_o \cos \theta}{(R_L + Z_o/2)^2 + X_L^2} \quad (2)$$

where  $R_L = \eta R_s$ , with  $\eta$  a loss factor defined for round wires as

$$\eta = g/2a \quad (3)$$

and  $R_s$  the surface resistivity, defined as  $R_s = \sqrt{\pi f \mu_o / \sigma}$ , given  $\sigma = 4.098 \times 10^7$  mho/m (Au) and  $\mu_o = 4\pi \times 10^{-7}$  H/m. This assumes the conductor depth is

$\gg \delta$ , the skin depth. For a plane mirror with negligible surface roughness (relative to  $\lambda$ ), the fraction of incident power absorbed is

$$A_m = \frac{P_{absorb}}{P_{incid}} = \frac{4R_s \cos \theta}{Z_o} \quad (4)$$

Figure 4 shows the power loss in dB from a single plane mirror and beam splitter grid across the receiver band. A value for  $R_s$  a factor of 2.2 higher than the above value is assumed, based on measurements by Batt *et. al.* [10] at  $\lambda=337 \mu\text{m}$ . The mirror loss is much lower than the loss from the grid; hence, there will not be a significant difference in overall loss between the two interferometer versions.

### 3.3 Dual-Beam Interferometer as an LO Diplexer

The dual-beam interferometers in Figures 1 and 2 are 4-port quasi-optical devices that can be used for LO diplexing or sideband separation, depending on the path length difference. As a diplexer, this path difference  $\Delta$  is

$$\Delta = (2K - 1)(\lambda_{IF}/2), \quad K = 1, 2, 3, \dots \quad (5)$$

where  $\lambda_{IF}$  is the wavelength at the center of the IF band. The power transmission in the signal path (Port 1 $\rightarrow$ 3), neglecting diffraction effects and ohmic losses, is given from [8] as

$$P_{SIG} = 1 - 2R(1 - R)[1 + \cos(2\pi\Delta/\lambda)] \quad (6)$$

where  $R$  is the fraction of incident power reflected off the wire grid. Nominally  $R=0.5$  at band center, but has a frequency dependence through  $X_L$ , given as

$$R = |1 + j2X_L/Z_o|^{-2} \quad (7)$$

Similarly, the power transmission in the LO path (Port 2 $\rightarrow$ 3) is given by

$$P_{LO} = 2R(1 - R)[1 + \cos(2\pi\Delta/\lambda)] \quad (8)$$

Given an ALMA IF center frequency of 8 GHz, the signal and LO transmission from Eqs. (6) and (8) is plotted across the receiver band in Figure 5. A value of  $K=1$  is used in Eq. (5); this yields the broadest bandwidth possible. The LO rejection is at a maximum near midband, but degrades toward the receiver band edges because of the frequency dependence of  $R$ .

### 3.4 Gaussian Beam Characteristics

The aperture size of the interferometer optics (i.e., splitters, lenses, mirrors) must be large enough to minimize the effects of beam truncation (vignetting) on the response. A general rule is to choose an aperture diameter at least *four* times the maximum beam radius. First, it will be useful to know the beam waist radius  $w_{cass}$  at the secondary focus. From [8],

$$w_{cass} = 0.22[T_{E,dB}]^{1/2}(f/D)\lambda \quad (9)$$

where  $T_{E,dB}$  is the edge taper in decibels and  $f/D$  the Cassegrain  $f/D$  ratio. For the ALMA antenna,  $T_{E,dB}=12$  dB and  $f/D=8$ , yielding a  $w_{cass}$  at 602 GHz of **3.04 mm**. Next, we will assume (for the moment) the maximum beam growth through the optics is equal to the beam radius at the confocal distance from the waist. This distance is calculated in [8] as

$$z_c = \pi w_{cass}^2 / \lambda = 58.3 \text{ mm} \quad (10)$$

with a corresponding beam radius of

$$w_{max} = \sqrt{2}w_{cass} = 4.30 \text{ mm} \quad (11)$$

Thus, the minimum (clear) beam aperture diameter should be  $4w_{max}$ , or **17.2 mm**. Applied to the interferometer in Figure 1, a 20 mm center-to-center spacing between the splitters implies that the minimum *unobstructed* path length difference can be no less than 40 mm. Unfortunately, with  $K=1$  in Eq. (5),  $\Delta$  is only 18.7 mm;  $K=2$  will increase  $\Delta$  to 56.2 mm, but at a 67% reduction in instantaneous IF bandwidth. The maximum path length through the diplexer for this case will be  $(\Delta + 2(20 \text{ mm}))$  or 96.2 mm, which is less than  $2z_c$ . Positioning the beam waist in the middle of this path will minimize beam truncation effects.

To obtain the maximum IF bandwidth without obstructing the beam, the interferometer configuration of Figure 2 can be used. The maximum path length in this diplexer for  $K=1$  as above will be  $(\Delta + 6(20 \text{ mm}))$  or 138.7 mm. Since this is greater than  $2z_c$ , significant beam truncation may occur unless the aperture is enlarged. However, doing this will increase the path length further, perhaps making things worse. To determine the optimal aperture size, the clear aperture of the Gaussian beam as a function of axial offset  $z$  from the beam waist is plotted beside the maximum beam splitter spacing that will satisfy the path length relation given above. The curves for the worst case ( $f=602$  GHz) are shown in Figure 6. Note that the confocal length calculated in Eq. (10) is below the crossing point of the two curves;

the beam will suffer truncation if the interferometer is built small enough to contain it within the limits  $\pm z_c$ . Nevertheless, the beam growth is still gradual at offsets well over  $z_c$ , and a significant increase splitter spacing not a problem as long as the clear aperture is above the corresponding minimum shown in the plot.

For example, if we assume a splitter separation 20% over the minimum clear aperture (to allow for the supporting frame of the wire grids), the maximum path length  $2z$  through the interferometer (Figure 7) works out to be 180 mm, corresponding to a splitter spacing of 26.9 mm, and a clear aperture no smaller than 22.4 mm.

### 3.5 Diffraction Effects

The process of splitting and recombining beams with a path length (phase) difference in the diplexer introduces an additional loss. This loss mechanism is due to higher-mode excitation when beams of unequal radii and radii of curvature are coupled, and is referred to as beam coupling loss or diffraction loss. From [8], the signal path gain including diffraction effects is given as

$$P_{SIG} = (1 - R)^2 + \frac{R^2}{1 + \alpha^2} - 2R(1 - R) \frac{\cos \gamma + \alpha \sin \gamma}{1 + \alpha^2} \quad (12)$$

where

$$\alpha = \frac{\lambda \Delta}{2\pi w_{cass}^2}, \quad \gamma = \frac{2\pi \Delta}{\lambda} \quad (13)$$

Note that for  $\alpha=0$ , Eq. (12) reduces to the the diffractionless case in Eq. (6). Likewise, for the LO path,

$$P_{LO} = R^2 + \frac{(1 - R)^2}{1 + \alpha^2} + 2R(1 - R) \frac{\cos \gamma + \alpha \sin \gamma}{1 + \alpha^2} \quad (14)$$

Figure 8 shows the signal and LO transmission response as in Figure 5, but includes diffraction effects. The plots are virtually identical, except that the response with diffraction is shifted slightly in frequency, and there is a small ( $\sim 0.067$  dB) loss in the passband. Null depth was unaffected; the frequency-dependent reactance of the grid wires has a far greater effect on the ultimate rejection.

### 3.6 LO Noise Rejection

The LO noise power injected into the desired signal band of the mixer is a function of the spectral noise power density  $\Phi_n$  of the LO source, the

diplexer gain in Eq. (14), the optics loss  $G_{op}$  and ambient temperature  $T_0$ , and is expressed as

$$P_n = \int_{f_1}^{f_2} G_{op} [P_{LO}\Phi_n + (1 - G_{op})kT_0] d\nu \quad (15)$$

where  $f_1$  and  $f_2$  are the band edge frequencies. For ALMA receivers this signal band is offset 4 to 12 GHz from  $f_{LO}$ ; at these carrier offsets the noise spectrum from either a multiplied Gunn oscillator or photonic LO source is essentially flat. Likewise, the loss in the lens and diplexer optics is nearly constant over the signal band. Given this, the equivalent temperature of the LO noise through the diplexer is

$$T_{eq} \simeq G_{op} \left[ T_0(1 - G_{op}) + \frac{T_{LO}}{f_2 - f_1} \int_{f_1}^{f_2} P_{LO} d\nu \right] \quad (16)$$

where  $T_{LO}$  is the equivalent noise temperature at the LO source and  $G_{op}$  is taken at the band center frequency  $f_c = (f_1 + f_2)/2$ .

The worst-case LO leakage into the signal band occurs at the upper edge of the receiver band, where the nulls in  $P_{LO}$  are not as deep (Figure 8). From Figure 4, the approximate ohmic loss at  $f_c=716$  GHz is  $\sim 0.20$  dB ( $G_{op}=0.96$ ), the total from two splitters and four mirrors. With the diplexer tuned to  $f_c$ , the resulting equivalent noise temperature over the entire 8 GHz IF band is

$$T_{eq} \simeq 12.6 + 0.207T_{LO} \quad (17)$$

assuming  $T_0=300$ K. Note that the constant term is independent of bandwidth, but still varies over frequency: it is  $\sim 2$ K higher at  $f_c=606$  GHz. For a Gunn source ( $T_{LO} \simeq 300$ K),  $T_{eq}=\mathbf{74.7K}$ .

By contrast, the best LO isolation is at mid-band, where  $R \simeq 0.5$  in the splitters. For the same 8 GHz bandwidth and  $T_{LO}$  as above the equivalent noise temperature is

$$T_{eq} \simeq 14.2 + 0.172T_{LO} = 65.8K \quad (18)$$

where  $G_{op}=0.95$ , and the same Gunn source above assumed.

In summary, the best LO rejection in the diplexer can be obtained by designing a splitter to minimize changes in the grid reactance  $X_L$  across the receiver band. Using thin strips instead of wires may improve the broadband performance of the grid splitter, but the dielectric backing necessary to support the structure will add to the loss. Second, the diplexer may need to be cooled to reduce to lower limit of  $T_{eq}$ , unless the loss in the splitters

can be further reduced by design. Finally, it should be noted that the equivalent LO noise temperature over a narrow segment of the signal band varies considerably across the band. While rejection can be quite good around the band center, there is virtually none at the edges.

## 4 Conclusions

The above analysis indicates that the interferometer configuration in Figure 2 is best, because of the broad IF bandwidth required by the ALMA. The critical element is the beam splitter: low ohmic loss and a grid reactance that is flat over the band will minimize thermal and LO noise injected into the mixers. Wire grids are fairly simple to construct and have very low cross polarization, but are not necessarily the best choice. Mirror loss is small, and given the relatively small beam diameters, optical-grade flat mirrors can be used, virtually eliminating surface scattering. Lastly, the diffraction loss is low, and has little if any effect on the shape of the diplexer response.

## 5 Acknowledgements

I would like to thank John Payne of NRAO for writing the introduction to this memo, and providing timely help and guidance. Thanks also to Bill Shillue of NRAO, for his many excellent suggestions and comments.

## References

- [1] A. R. Thompson and L. R. D'Addario, "Relative Sensitivity of Double- and Single-Sideband Systems for both Total Power and Interferometry", *ALMA Memo 304*, NRAO, Socorro NM, 2000
- [2] J. W. Lamb, "SSB vs. DSB for Submillimeter Receivers", *ALMA Memo 301*, NRAO, Socorro NM, 2000
- [3] P. R. Jewell and J. G. Mangum, "System temperatures, Single Versus Double Sideband Operation, and Optimum Receiver Performance", *MMA Memo 170*, NRAO, Socorro NM, 1997
- [4] A. R. Thompson and A. R. Kerr, "Relative Sensitivities of Single and Double Sideband Receivers for the MMA", *MMA Memo 168*, NRAO, Socorro NM, 1997



- [5] A. R. Kerr, ALMA Receiver Meeting, Charlottesville VA, April 2000
- [6] J. M. Payne and M. R. Wordeman, "Quasi-optical diplexer for millimeter wavelengths", *Rev. Sci. Instrum.*, 49(12), Dec. 1978, pp. 1741-1743
- [7] J. M. Payne, J. E. Davis and M. B. Hagstrom, "Dual polarization quasi-optical beam divider and its application to a millimeter wave diplexer", *Rev. Sci. Instrum.*, 53(10), Oct. 1982, pp. 1558-1560
- [8] P. Goldsmith, "Quasi-Optical Techniques", *Infrared and Millimeter Waves*, Vol. 6, Academic Press, 1982, pp.277-343
- [9] N. Marcuvitz, *Waveguide Handbook*, MIT Radiation Laboratory Series, Vol. 10, McGraw-Hill, New York, 1951, Sec. 5-21, p. 286
- [10] R. Batt, G. Jones and D. Harris, "The measurement of the surface resistivity of evaporated gold at 890 GHz", *IEEE Trans. Microwave Theory Tech.*, MTT-25, 1977, pp. 488-491

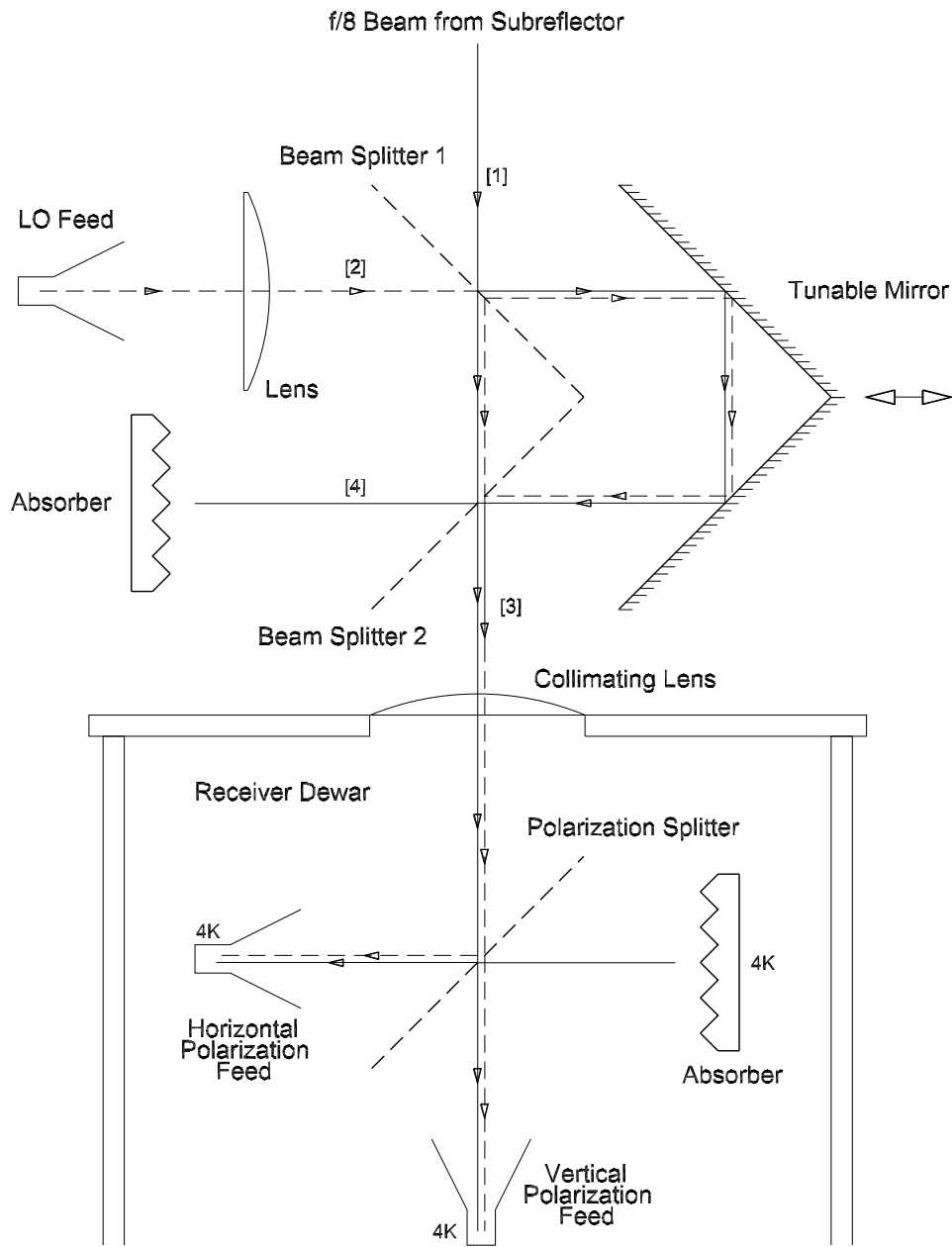


Figure 1: Dual-Polarization Double Sideband (DSB) Receiver Optics (1)

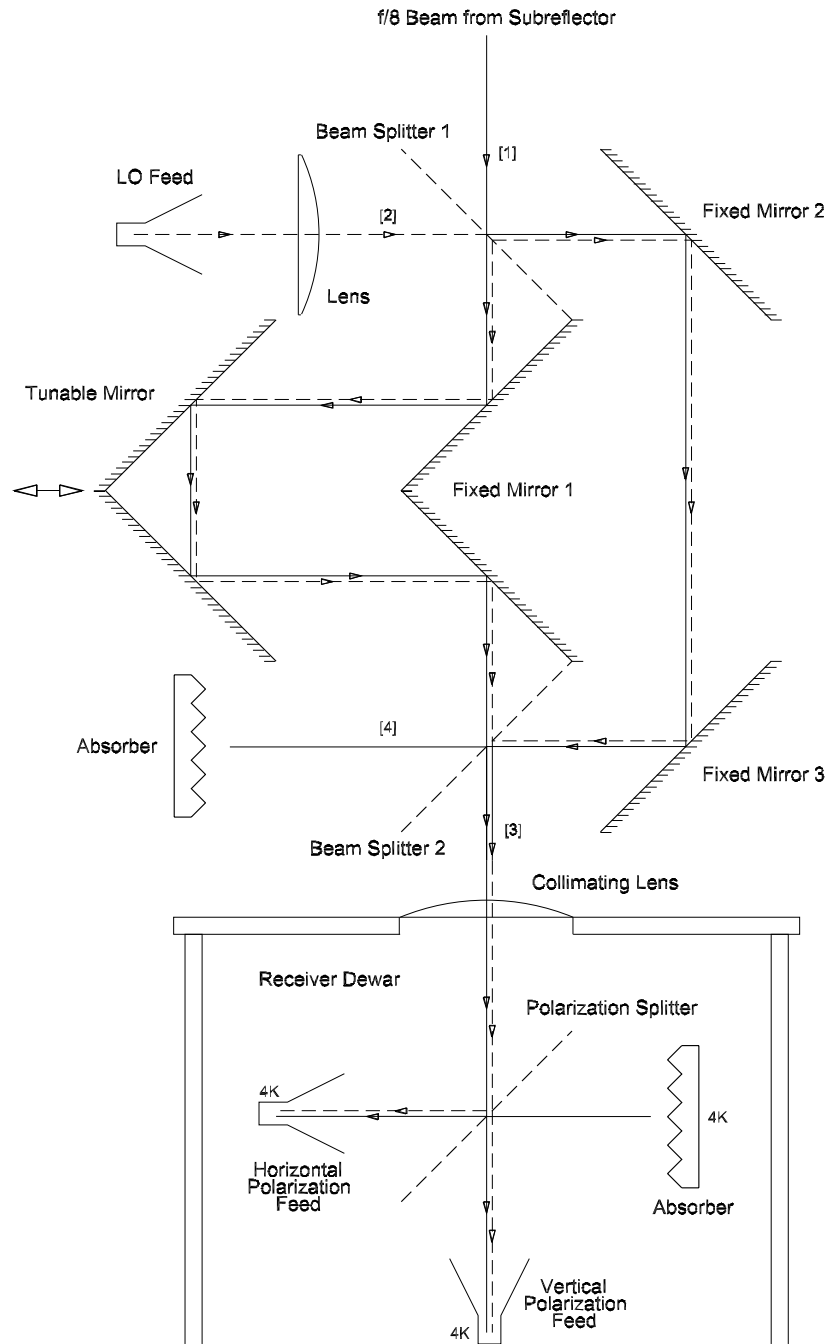


Figure 2: Dual-Polarization Double Sideband (DSB) Receiver Optics (2)

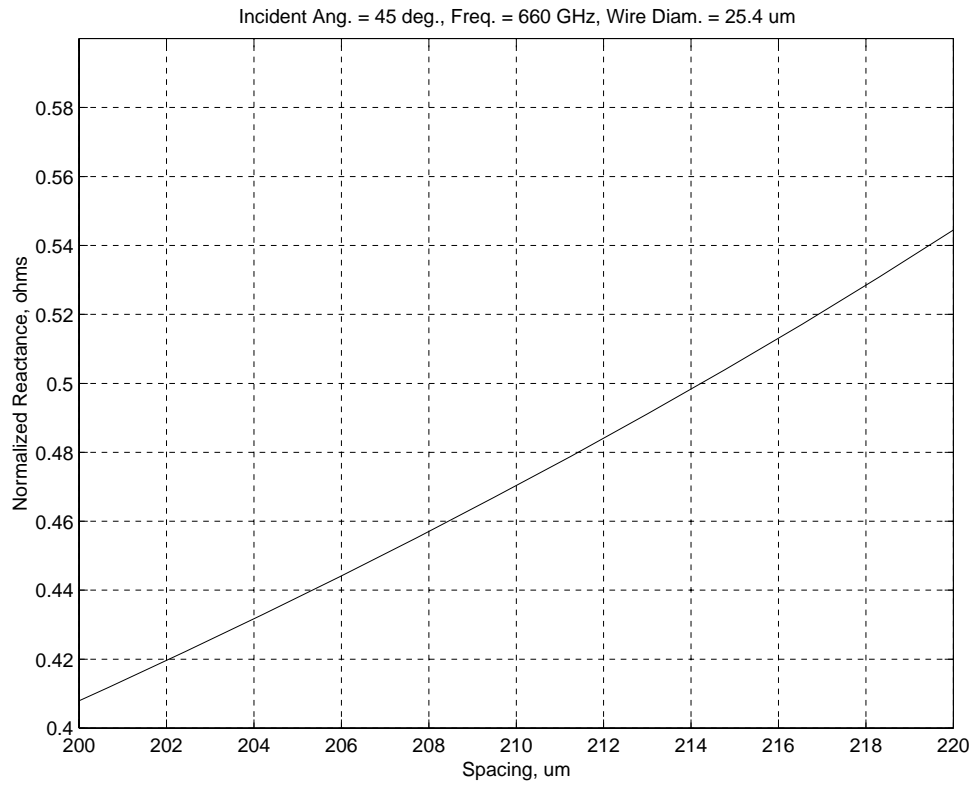


Figure 3: Splitter Grid Inductance vs. Wire Spacing

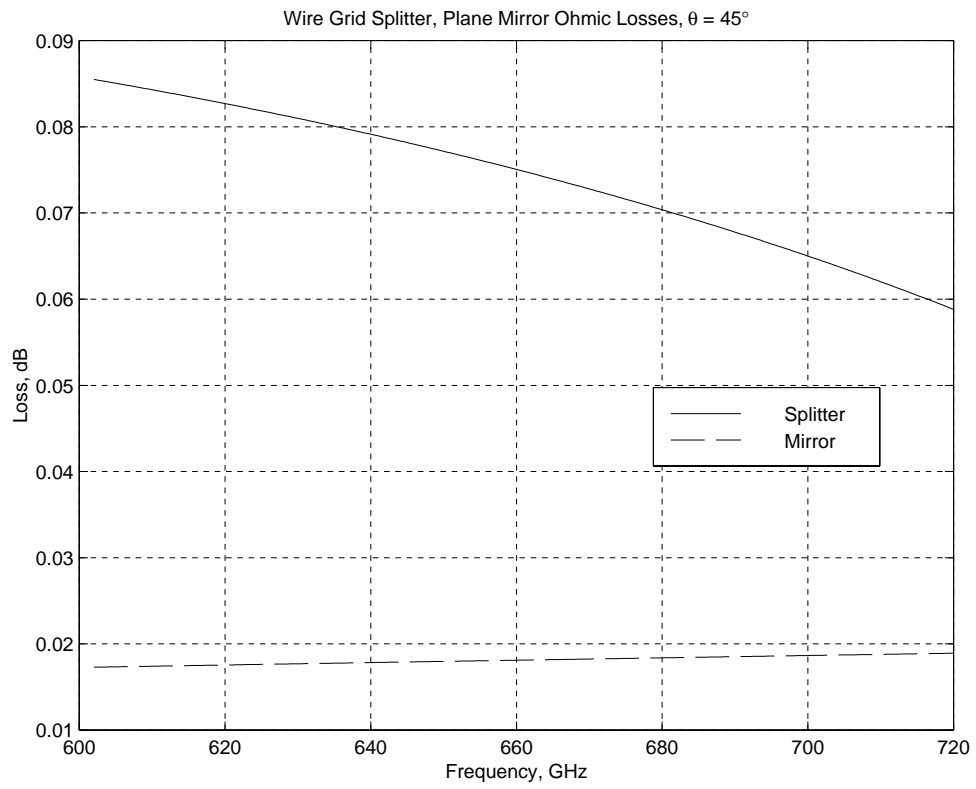


Figure 4: Beam Splitter Grid and Mirror Loss vs. Frequency

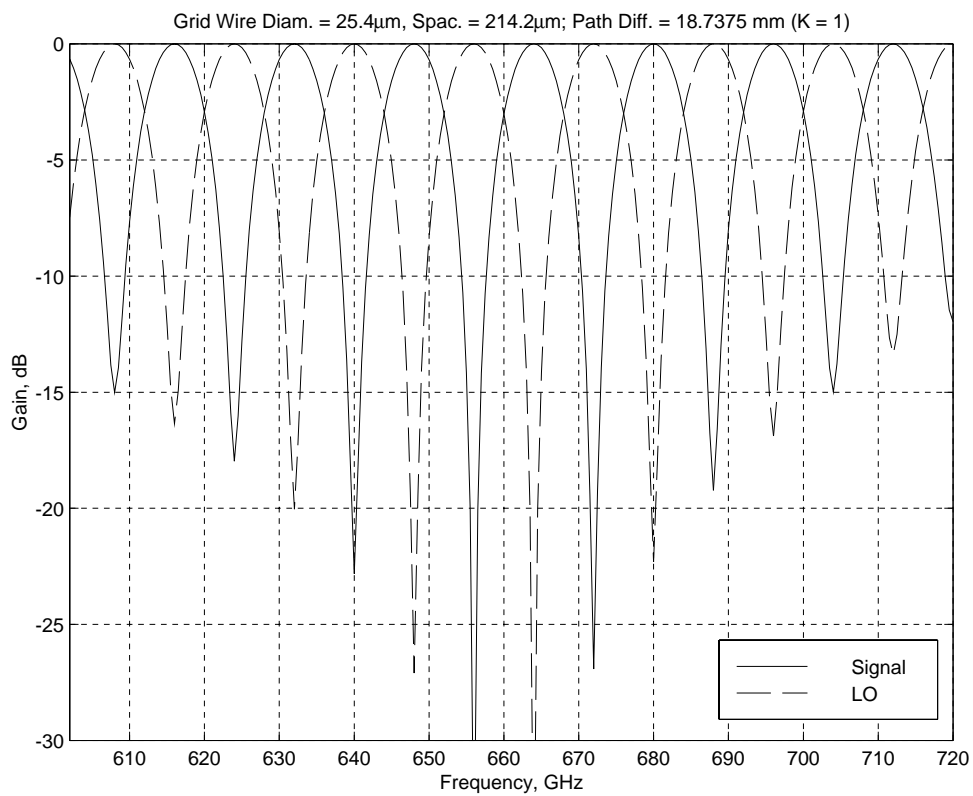


Figure 5: Diplexer Insertion Loss vs. Frequency

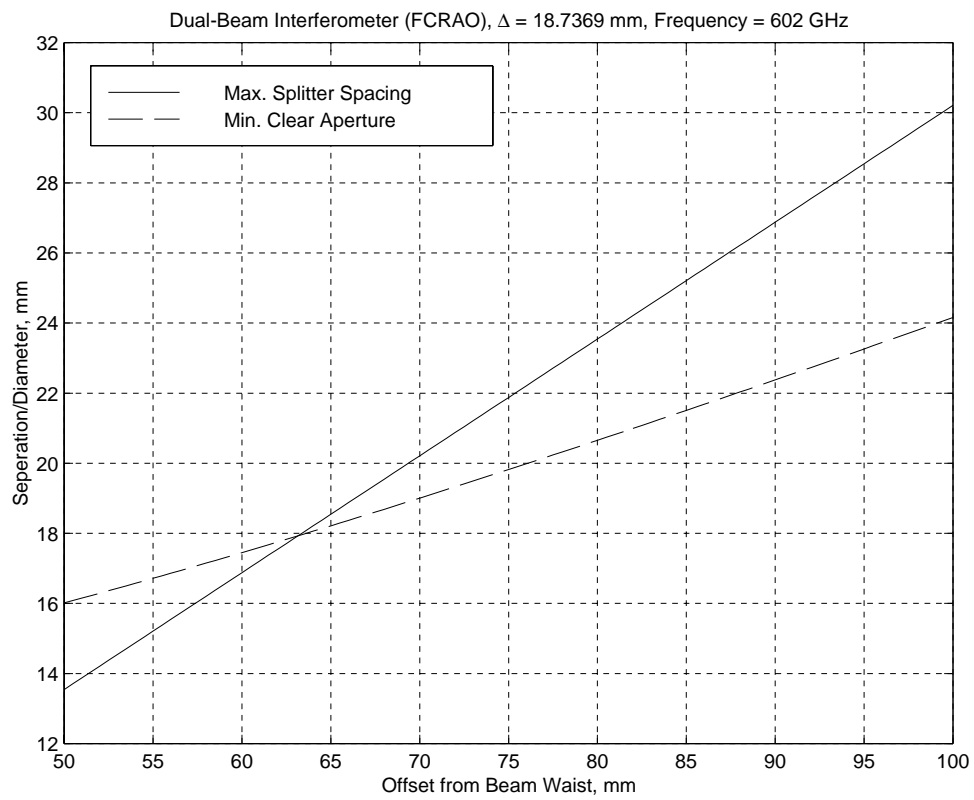


Figure 6: Min. Beam Aperture and Max. Splitter Separation vs.  $z$

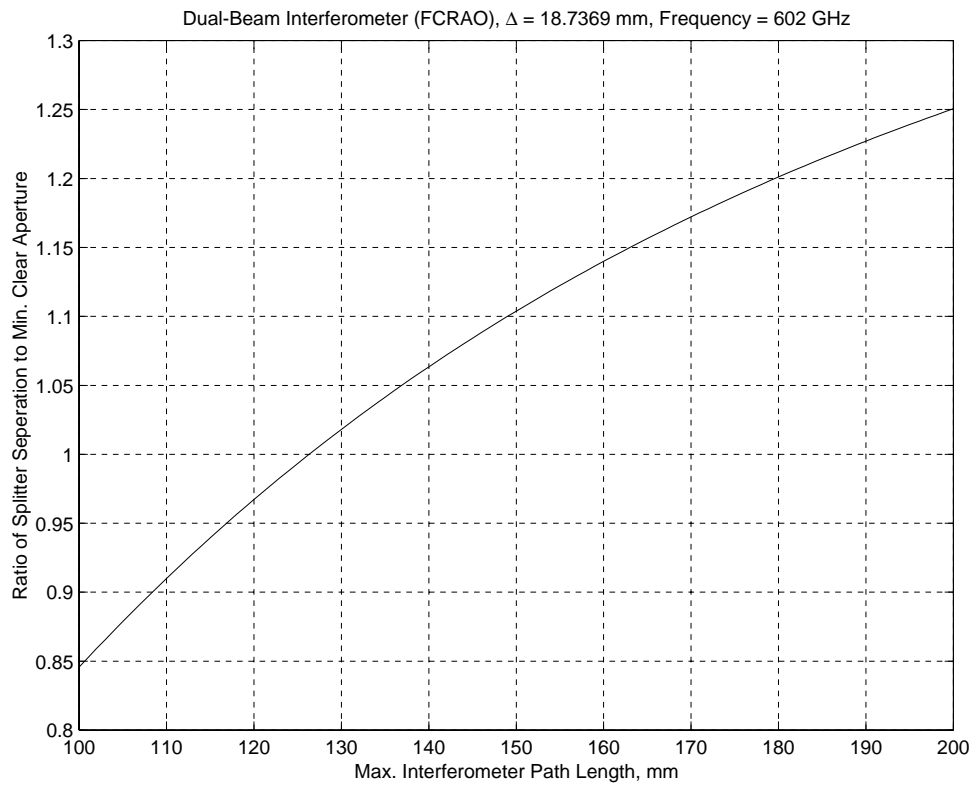


Figure 7: Ratio of Splitter Separation to Min. Clear Aperture, vs.  $2z$



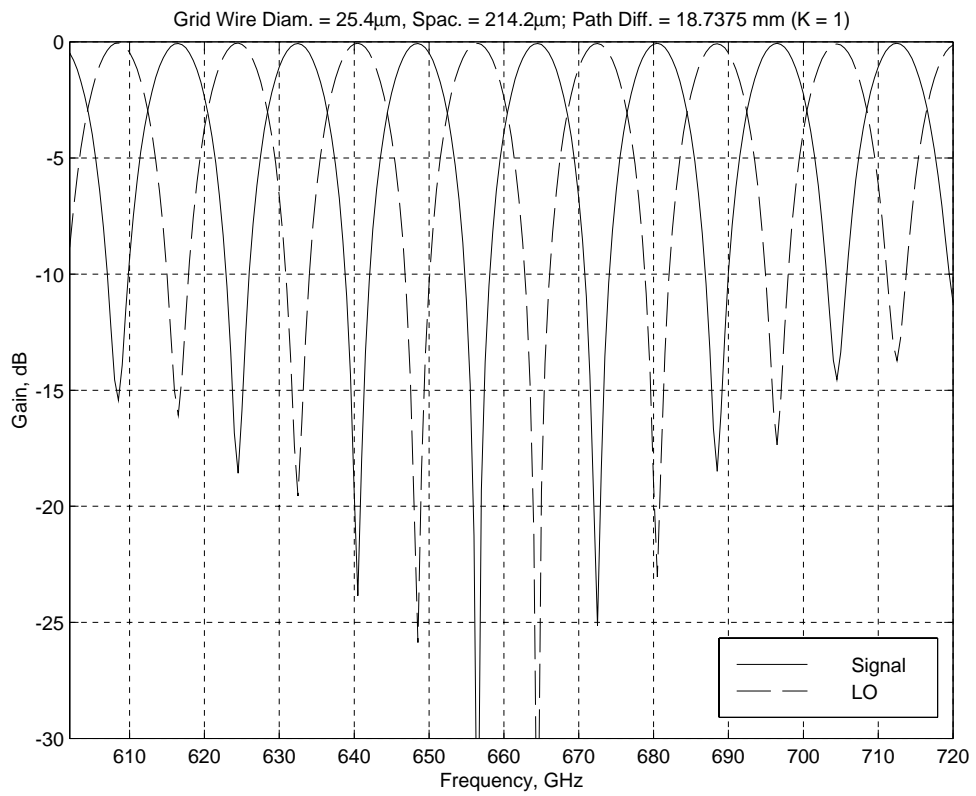


Figure 8: Diplexer Insertion Loss vs. Frequency, with Diffraction Effects